JOURNAL OF SOLID STATE CHEMISTRY 113, 78–87 (1994)

Microstructural Characterization of $BaMnO_{3-y}$ ($0.08 \leq y \leq 0.12$): Evidence for a New Polytype (21R)

M. Parras,* J. M. González-Calbet,*·†·[1] J. Alonso,*·† and M. Vallet-Regí†·‡

*Departmento de Química Inorgánica, Facultad de Químicas, Universidad Complutense, 28040 Madrid, Spain; †Instituto de Magnetismo Aplicado (RENFE-UCM), Apdo. 155, 28230 Las Rozas, Madrid, Spain; and ‡Departmento de Química Inorgánica y Bioinorgánica, Facultad de Farmacia, Universidad Complutense, 28040 Madrid, Spain

Received August 10, 1993; in revised form December 6, 1993; accepted December 7, 1993

Compositional variations in $BaMnO_{3-y}$ perovskite-related materials in the $0.08 \leq y \leq 0.12$ range are accommodated either by means of the formation of an ordered rhombohedral phase for $y = 0.10$ (15R type) or by means of disordered intergrowths of both 15R and a new polytype of nominal composition $BaMnO_{2.928}$. This phase can be described as formed by 21 layers per unit cell, following the stacking sequence . . . $(chhhhhh)_3$ . . . .

INTRODUCTION

The $BaMnO_3$ perovskite-related oxide crystallizes in the 2H structural type. This type can be described as formed by a hexagonal sequence (. . . hhh . . .) of BaO_3 layers (1). Powder X-ray diffraction (XRD) data performed by Negas and Roth (2) have shown a series of different phases in the anion-deficient $BaMnO_{3-y}$ system ($0 \leq y \leq 0.25$): a rhombohedral 15-layer-type, $(chhhh)_3$ stacking sequence and hexagonal 8H, . . . $(hhhc)_2$. . . , 6H, . . . hchhhc . . . , 10H, . . . $(hhchc)_2$ . . . , and 4H, . . . hchc . . . , types.

In a series of previous papers (3, 4), it has been stated that, in the reduction process of $BaMnO_3$, the oxygen deficiency is accommodated by means of the introduction of $BaO_{2.50}$ cubic layers. Since BaO_3 is the composition for a hexagonal layer, the ideal anionic composition for every hexagonal type can be established: $BaMnO_3$ (2H), $BaMnO_{2.90}$ (15R), $BaMnO_{2.875}$ (8H), $BaMnO_{2.833}$ (6H), $BaMnO_{2.80}$ (10H), and $BaMnO_{2.75}$ (4H). According to this, it seems that the first condition for obtaining one of these structural types is that the anionic composition has to be coincident with the ideal composition corresponding to every structural type.

Moreover, probably due to the very close anionic composition shown by these phases, the synthetic route also plays an important role in order to isolate $BaMnO_{3-y}$ phases. We have shown (3) that only when the reduction process is performed starting from a well-ordered $BaMnO_3$ sample can a single phase be obtained.

If one of these conditions (ideal composition and ordered starting material) is not observed, nonstoichiometry is accommodated by means of disordered intergrowths of both cubic and hexagonal layers.

We show, in this paper, an electron diffraction and microscopy study of the $BaMnO_{3-y}$ system in the $0 < y \leq 0.12$ compositional range, where, up to now, only the 15R phase has been reported.

EXPERIMENTAL

The $BaMnO_3$ (2H-type) starting material was obtained by heating stoichiometric amounts of $BaCO_3$ and $MnCO_3$ at 980°C for 48 hr ($pO_2 = 0.2$ atm). Both powder X-ray and electron diffraction patterns can be indexed on the basis of an ordered 2H structural type of parameters $a = 0.57$ nm and $c = 0.48$ nm. Annealing of this material at various temperatures leads to the following compounds:

$T = 1250$°C (5 days) : $BaMnO_{2.92}$
$T = 1275$°C (5 days) : $BaMnO_{2.90}$
$T = 1300$°C (3 days) : $BaMnO_{2.88}$.

The above oxygen content has been determined by thermogravimetric analysis developed on the basis of a Cahn D-200 electrobalance. The samples were reduced under H_2 atmosphere at 800°C. Since the final product of the reduction process was always the same mixture of Ba and Mn oxides, the oxygen content was established from the weight difference between the starting and the final products. These results are compared to those obtained for stoichiometric 2H $BaMnO_3$ reduced under identical conditions.

[1] To whom correspondence should be addressed.

0022-4596/94 $6.00

Powder X-ray diffraction (XRD) was carried out on a SIEMENS D-5000 diffractometer with a graphite monochromator and using Cu$K\alpha$ radiation.

Selected-area electron diffraction (SAED) and electron microscopy were carried out on a JEOL 2000FX electron microscope. High-resolution electron microscopy (HREM) was performed on a JEOL 4000EX electron microscope.

RESULTS AND DISCUSSION

Powder XRD corresponding to both $BaMnO_{2.92}$ and $BaMnO_{2.90}$ samples are shown in Figs. 1a and 1b, respectively. The $BaMnO_{2.88}$ sample shows a powder XRD similar to that shown for $BaMnO_{2.90}$. All diffraction maxima can be indexed on the basis of a unit cell of rhombohedral symmetry characteristic of the 15R structural type. However, some differences are observed: the relative intensity of some reflections (for instance, $(107)_h$ and $(018)_h$) is different, comparing both diagrams, and a broadening of the maxima is detected in the $BaMnO_{2.92}$ sample.

In order to solve such differences, a SAED and HREM study was performed.

Microstructural Characterization of $BaMnO_{2.90}$

Figure 2 shows the SAED pattern (Fig. 2a) and the corresponding HREM image (Fig. 2b) of a well-ordered crystal along the $[100]_h$ zone axis. The SAED pattern only shows the (hkl) reflections with $-h+k+l = 3n$, which confirms the symmetry deduced from the XRD pattern. In the HREM image it can be observed that the d spacing along the c-axis is 3.5 nm, which corresponds to 15 BaO_x layers per hexagonal unit cell. Moreover, from the different contrast observed in the HREM image, the $(chhhh)_3$ stacking sequence corresponding to the 15L structural type, previously described by Negas and Roth (2), can be detected.

Figure 2c shows a representation of the structural model projected along the $[100]_h$ direction from which a direct comparison between the ideal and the experimental structural features could be established. Image calculations (Fig. 2d) of such a model were performed using the multislice method (5), under the following conditions: sample thickness (t) at 5 and 6 nm; $\Delta f = -60$ and -70 nm. The best fit seems to be obtained for $t = 5$ nm and $\Delta f = -70$ nm. Although very small differences are observed, this is because image calculations have been carried out considering a BaO_3 stoichiometry in every layer on the basis of an ideal sequence of 15 layers.

Taking into account that the anionic composition per cubic layer is $BaO_{2.50}$, while BaO_3 is the corresponding composition for a hexagonal layer, the ideal composition for this ordered structural type is $BaMnO_{2.90}$ per unit formula, in agreement with the experimental composition obtained by thermogravimetry.

It should be mentioned that a certain amount of crystals ($\simeq$10%) were twinned as shown in the electron diffraction pattern depicted in Fig. 3. Effectively, this SAED pattern can be interpreted as the superposition of two domains corresponding to the 15L structural type related to each other by a 180° rotation.

Microstructural Study of $BaMnO_{2.92}$

Figures 4a and 4b show the SAED pattern and the corresponding HREM image along $[100]_h$, respectively. The streaking along the c^*-axis in the diffraction pattern is reflected in the structural disorder observed in the image. Two different d spacings are mainly detected along the c-axis: $d = 1.16$ and 1.63 nm, which correspond to 5 and 7 BaO_x layers, respectively.

Figure 5 shows an enlargement of Fig. 4b. On the basis of the different contrast observed (3), the stacking sequence corresponding to the previous d spacings can be deduced:

5 layers: . . . chhhh . . .
7 layers: . . . chhhhhh . . . .

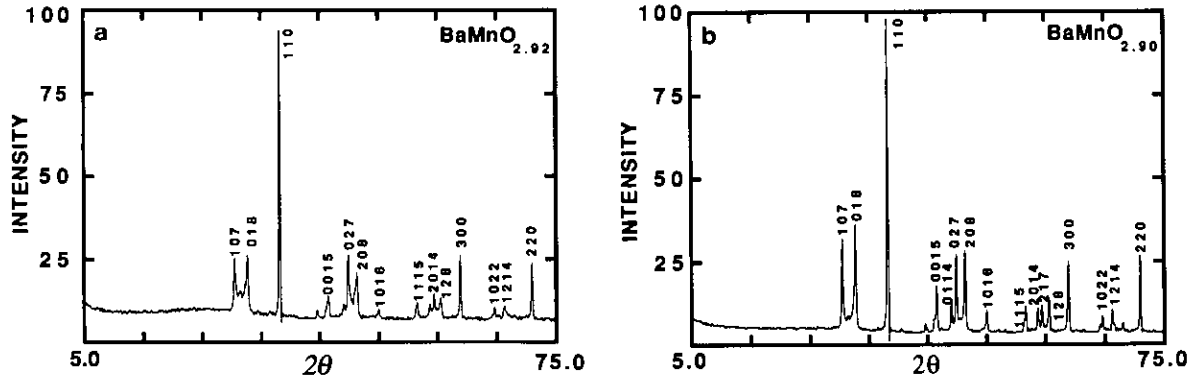

FIG. 1. Powder X-ray diffraction patterns, indexed according to a hexagonal setting, corresponding to (a) sample $BaMnO_{2.92}$ and (b) sample $BaMnO_{2.90}$.

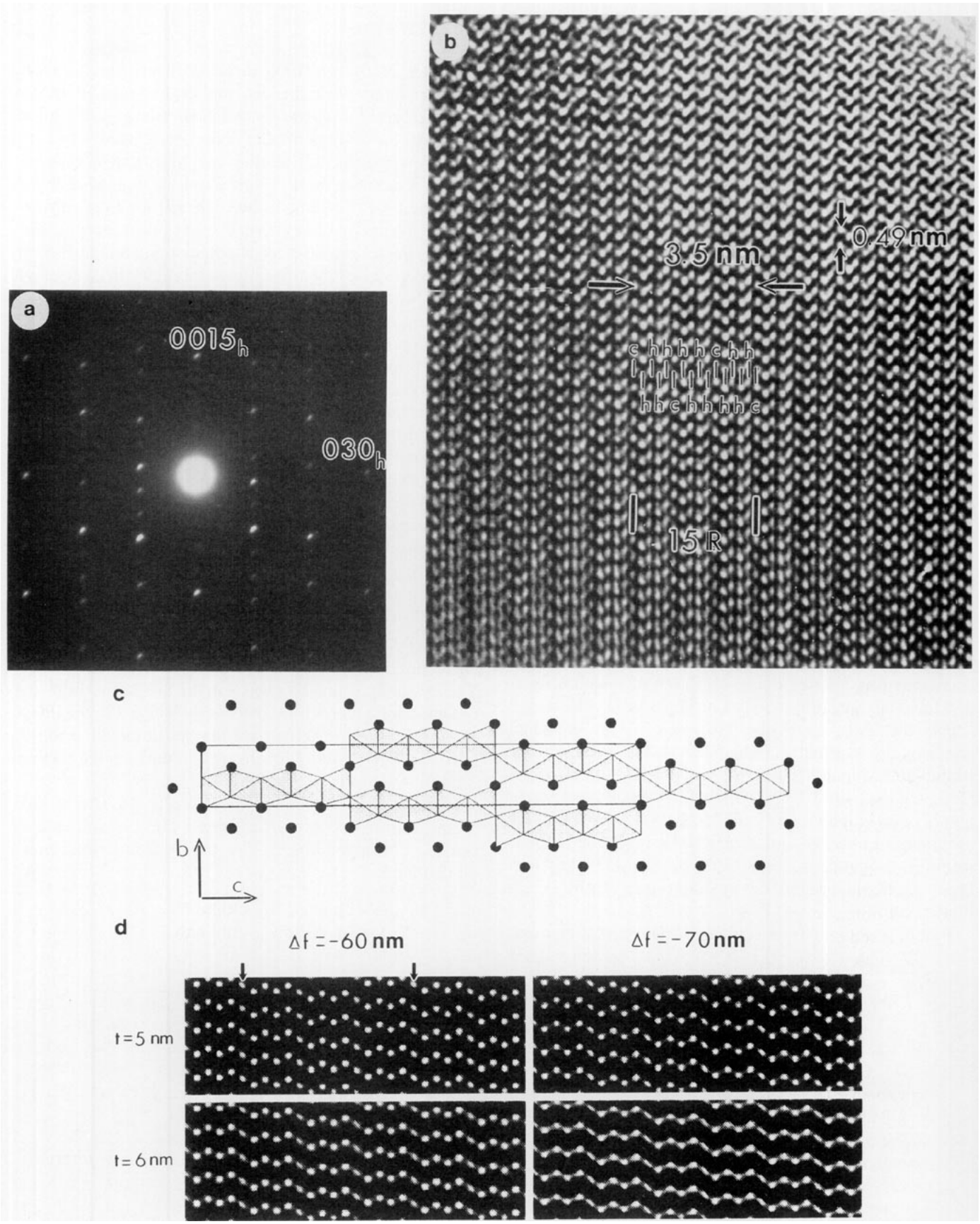

FIG. 2. (a) SAED pattern along $[100]_h$, corresponding to $BaMnO_{2.90}$. (b) Corresponding HREM image. The $(chhhh)_3$ stacking sequence is marked. (c) 15R structural model along the $[100]_h$ projection, with the $R\bar{3}m$ space group. The unit cell is outlined. (d) Calculated images on the basis of an ideal 15R structural type along $[100]_h$. Arrows indicate the c-axis value.

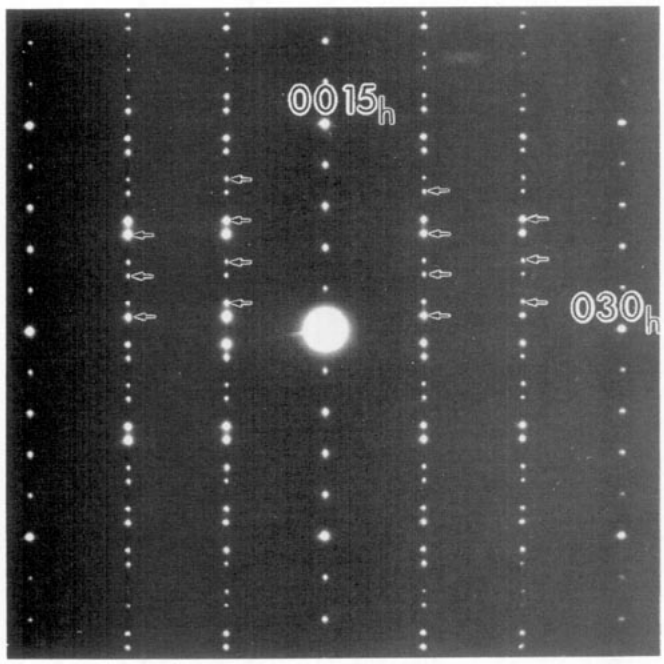

FIG. 3. SAED pattern along $[100]_h$ of a twinned crystal of sample $BaMnO_{2.90}$. Arrows indicate spots corresponding to the component tilted at 180°. Both (001)* and (031)* reflections are coincident.

The first stacking sequence corresponds to the 15R structural type, although sometimes only five layers of this polytype are observed: 1/3 15R.

The 7-layer sequence along the c-axis should correspond, according to Zhdanov (6), to 1/3 of a new polytype showing rhombohedral symmetry (space group $R\bar{3}m$), i.e., 21 layers per hexagonal unit cell.

One unit cell of such a structural type with $d \approx 4.9$ nm is clearly observed in Fig. 5. The Fourier transform calculated on this area confirms the rhombohedral symmetry. Effectively, the optical diffraction pattern of such a unit cell obtained by means of a CCD camera (Fig. 6) can be indexed on the basis of the rhombohedral unit cell.

Since isolated lamellae of the 21R type were frequently observed in a majority of disordered crystals, an exhaustive examination of this sample was performed. A fraction of crystals was indexed on the basis of the previously described 15R structural type. However, another minor fraction of crystals presented the electron diffraction pattern shown in Fig. 7a. Although weak streaking is observed, all diffraction maxima can be indexed on the basis of a 21R-type structure along $[100]_h$. The corresponding eleetron micrograph (Fig. 7b) shows a nearly ordered material with d spacing of 4.9 nm, which corresponds to 21 layers along the c-axis.

By supposing an ideal 21R sequence with $R\bar{3}m$ symmetry, the corresponding atomic positions are 3 Ba in (a); 6 Ba in (c), $z \approx 2/21$; 6 Ba in (c), $z \approx 4/21$; 6 Ba in (c), $z \approx 6/21$; 3 Mn in (b); 6 Mn in (c), $z \approx 15/42$; 6 Mn in (c), $z \approx 17/42$; 6 Mn in (c), $z \approx 19/42$; 9 O in (e); 18 O in (h), $x \approx 1/6$, $z \approx 1/21$; 18 O in (h), $x \approx 1/2$, $z \approx 2/21$; 18 O in (h), $x \approx 1/6$, $z \approx 3/21$.

The corresponding structural model along $[100]_h$ is shown in Fig. 8. This structure can be described as a sequence of three sets of seven octahedra sharing faces, which are linked sharing corners along the c-axis.

From the ideal atomic coordinates, the powder X-ray diffraction pattern has been calculated by the Rietveld method (7). By comparing this pattern with the calculated one for the 15R structure type (Fig. 9), it can be observed that diffraction maxima appear, in both phases, at d spacings very close, although some differences in the relative intensity of the reflections can be appreciated. This explains why the 21R phase has not been detected in the experimental XRD pattern shown in Fig. 1. In fact, all the diffraction maxima appearing in the experimental pattern could be indexed, in a first approximation, on the basis of the 15R structural type, but, after discovering the 21R structure type, they could also be assigned to this phase. However, the bad quality of the diffraction pattern is a consequence of the presence of a disordered material due to the majority presence of disordered intergrowths of both 15R and 21R polytypes.

Coming back to the ideal composition corresponding to cubic ($BaO_{2.50}$) and hexagonal (BaO_3) layers, the chemical composition for the 21R structural type should be $BaMnO_{2.928}$ per unit cell. Since the experimental composition obtained for this sample is $BaMnO_{2.92}$, new attempts will be devoted to isolate this material as a single phase.

Microstructural Characterization of $BaMnO_{2.88}$

Most of crystals show the SAED pattern along $[100]_h$ appearing in Fig. 10a. Diffraction maxima can be indexed on the basis of a 15R rhombohedral unit cell. Some streaking along c^* is apparent as reflected in the corresponding image. Figure 10b shows a low-resolution micrograph, where a unit cell of the 21R structure type is intergrown in a 15R matrix. Note that in spite of the close structural relationship between all the $BaMnO_{3-y}$ structural types, only polytypes showing rhombohedral symmetry seem to intergrow together inside a same crystal. In addition, when structural disorder is observed in a hexagonal type, this is only constituted by structural types showing hexagonal symmetry (see Fig. 2 of Ref. (4)).

Moreover, a small fraction of crystals shows the SAED pattern depicted in Fig. 11. This pattern can be interpreted as the $[100]_h$ projection of an eight-layer hexagonal type. Since no extinctions characteristic of the $P6_3/mmc$ space group are encountered, this crystal could be assigned to the $P\bar{6}m2$ space group. This suggests that this kind of crystal shows the $8H'$-type stacking sequence, . . .

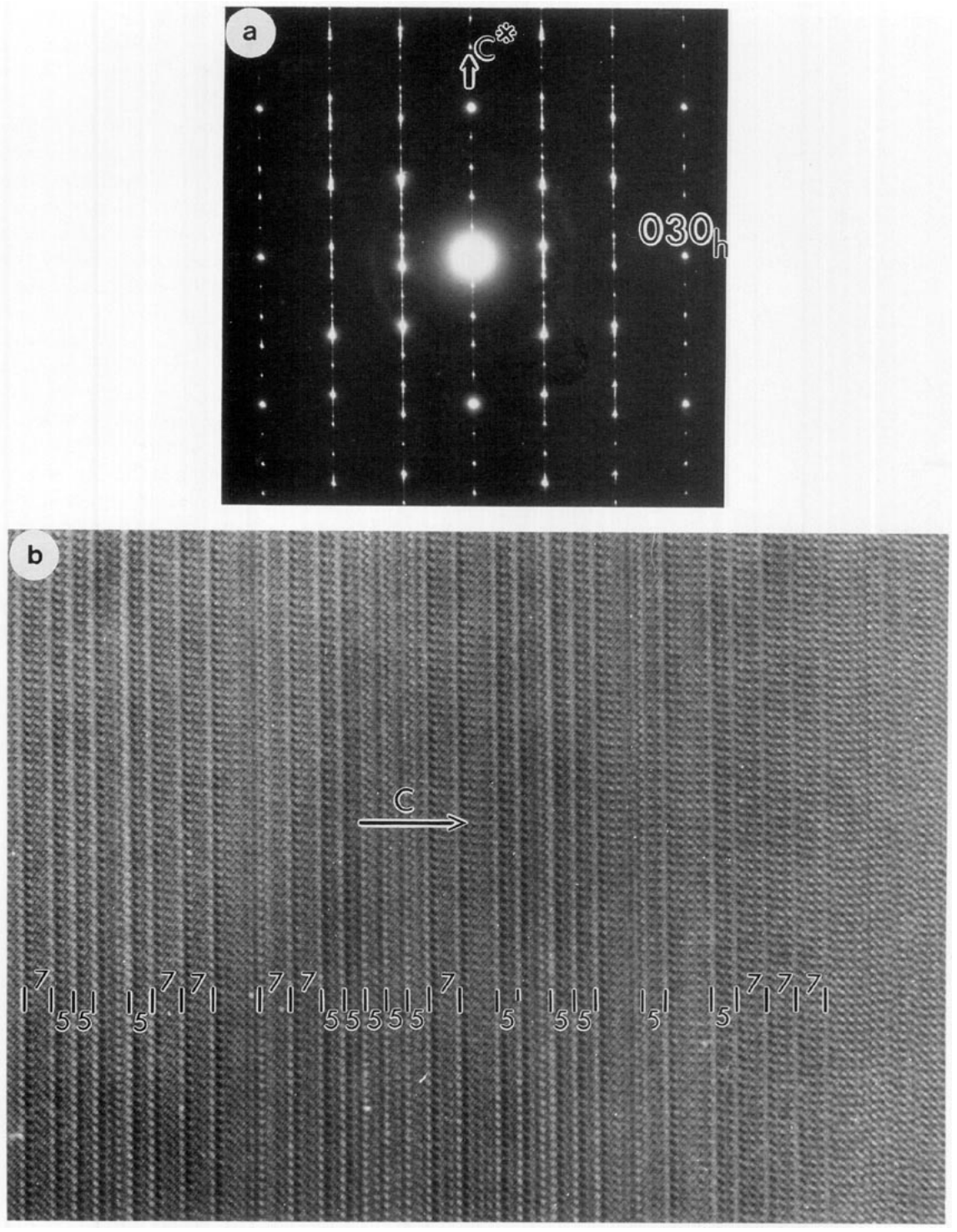

FIG. 4. (a) SAED pattern along $[100]_h$ of a crystal corresponding to sample $BaMnO_{2.92}$. Streaking along c^* is apparent. (b) corresponding electron micrograph showing disordered intergrowths between two polytypes.

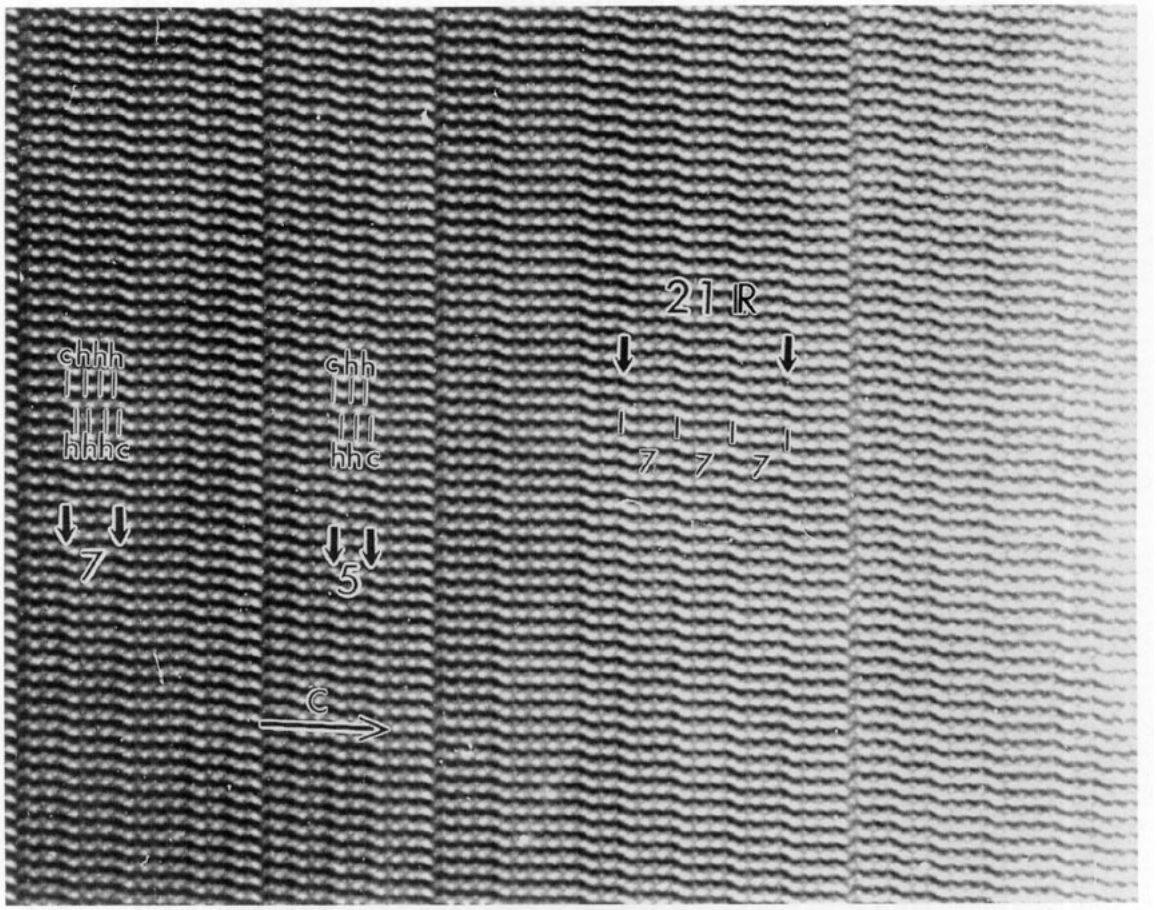

FIG. 5. Enlargement of Fig. 4b. The stacking sequence for both five and seven layers is marked. A 21R-type unit cell is marked.

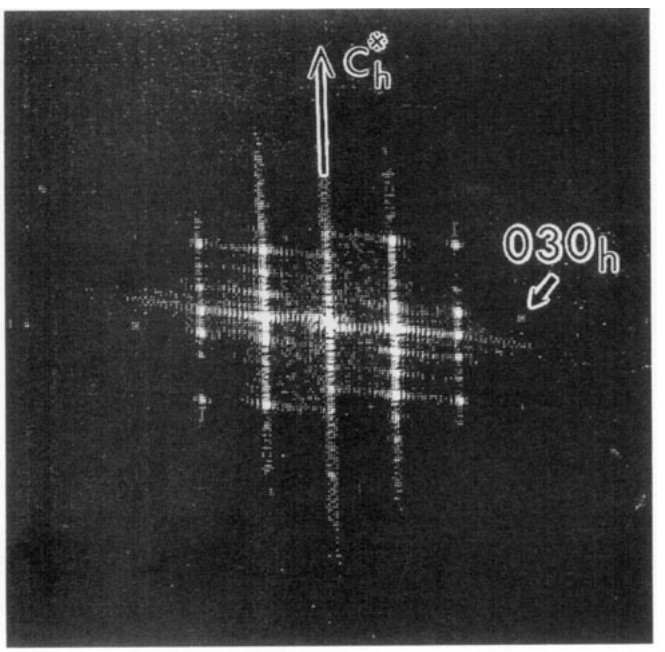

FIG. 6. Fourier transform of a 21R-type unit cell.

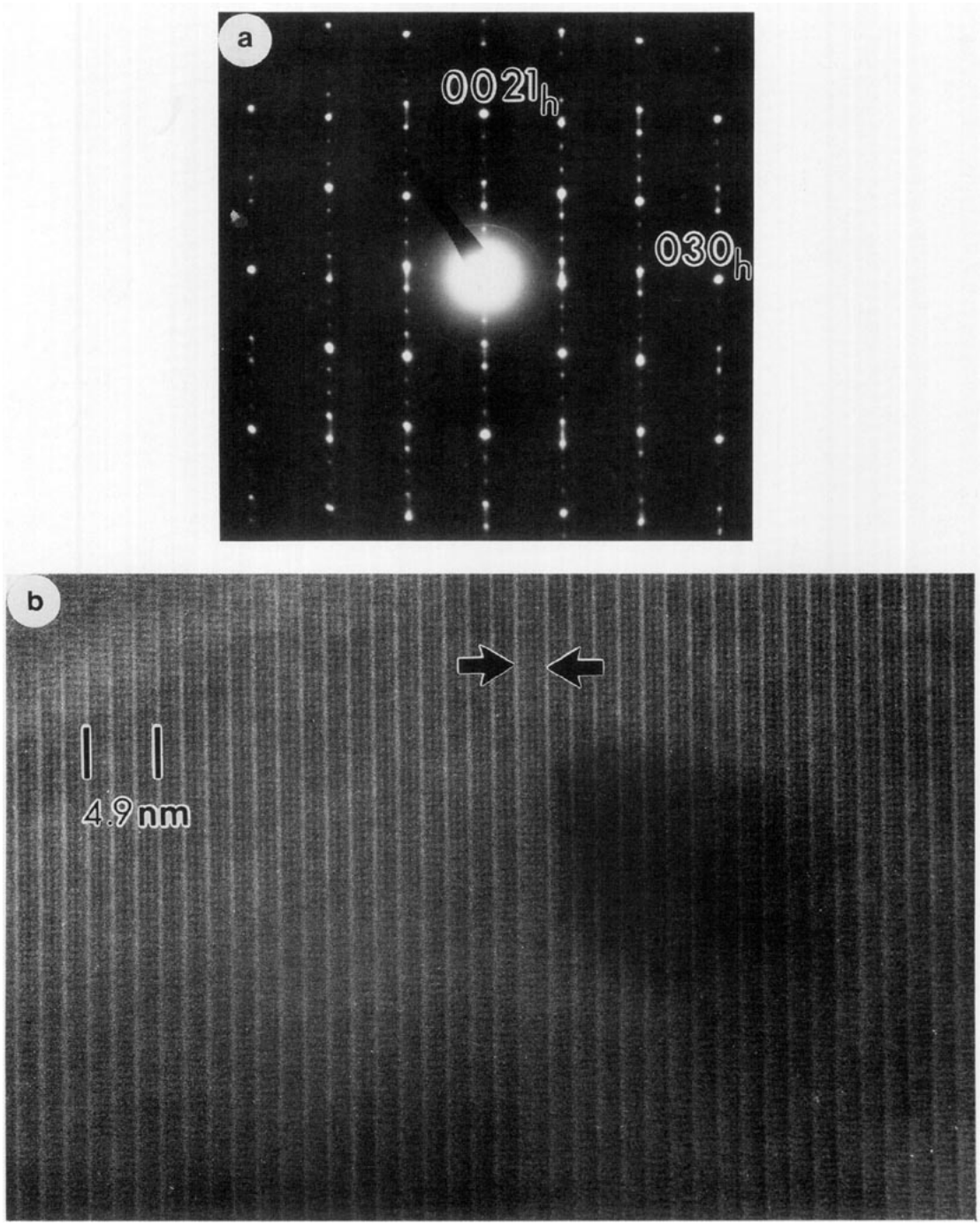

FIG. 7. (a) SAED pattern along $[100]_h$, corresponding to a 21R-type crystal. Weak streaking along the c^*-axis is apparent. (b) Corresponding low-resolution image showing crystallographic planes, with $d \simeq 4.9$ nm. A structure defect corresponding to a sequence of nine hexagonal layers is marked with arrows.

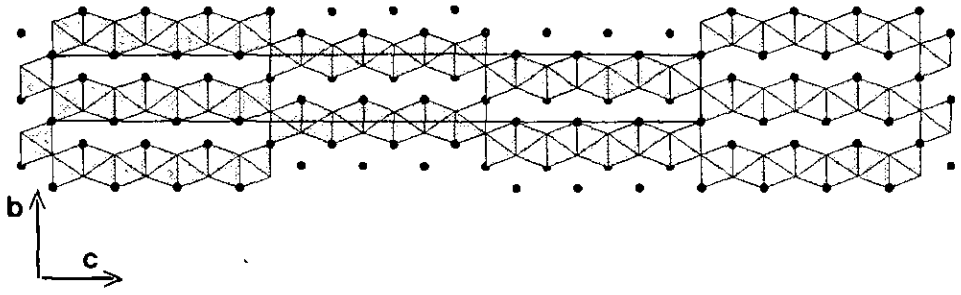

FIG. 8. 21R structural model along the $[100]_h$ projection with $R\bar{3}m$ symmetry. The unit cell is outlined.

chhhhhch . . . , described in Ref. (4), rather than the 8H-type stacking sequence, . . . $(chhh)_2$ . . . , proposed by Negas and Roth (2).

Finally, another minority fraction of crystals showing a well-ordered 15R structure type was detected.

On the basis of the experimental results obtained in such a narrow compositional range, $0.08 \leq y \leq 0.12$, some interesting aspects can be noted. First, the 15R structural type is by far the most abundant phase in this compositional range. However, it seems quite difficult to obtain a 15R single phase, since many times it appears intergrown with the related 21R structural type. Only when the experimental composition corresponds to the theoretical stoichiometry of this type, i.e., $BaMnO_{2.90}$, are practically the total amount of crystals ordered. Small deviations of this composition are accommodated by means of disordered intergrowths of this polytype with a new type, 21R, also showing rhombohedral symmetry. The theoretical composition corresponding to the 21R phase is 2.928, and, in fact, when the experimental composition is close to

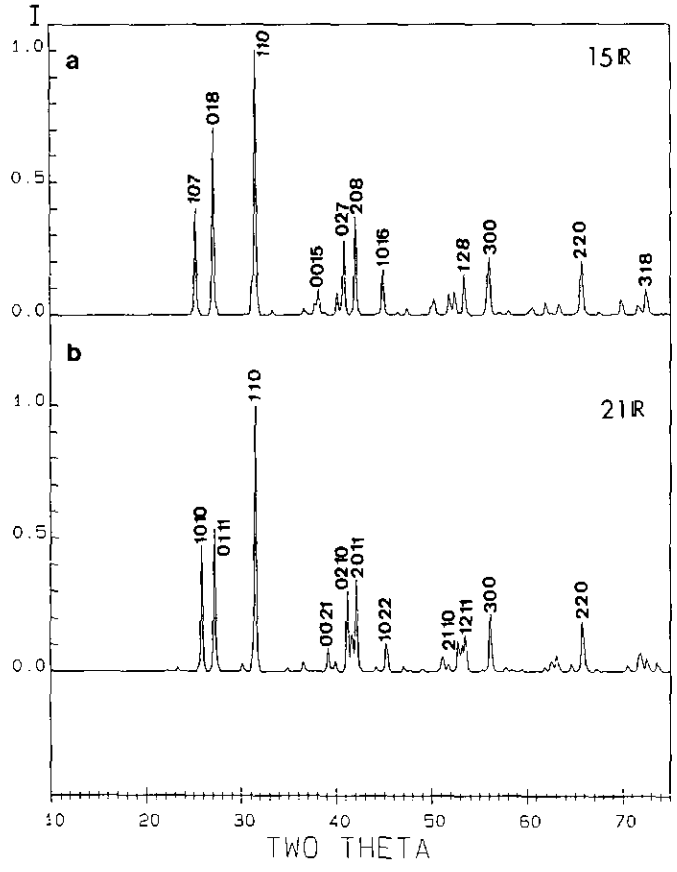

FIG. 9. Calculated powder X-ray diffraction patterns indexed according to a hexagonal setting for (a) 15R and (b) 21R structural types. Only strong reflections have been marked.

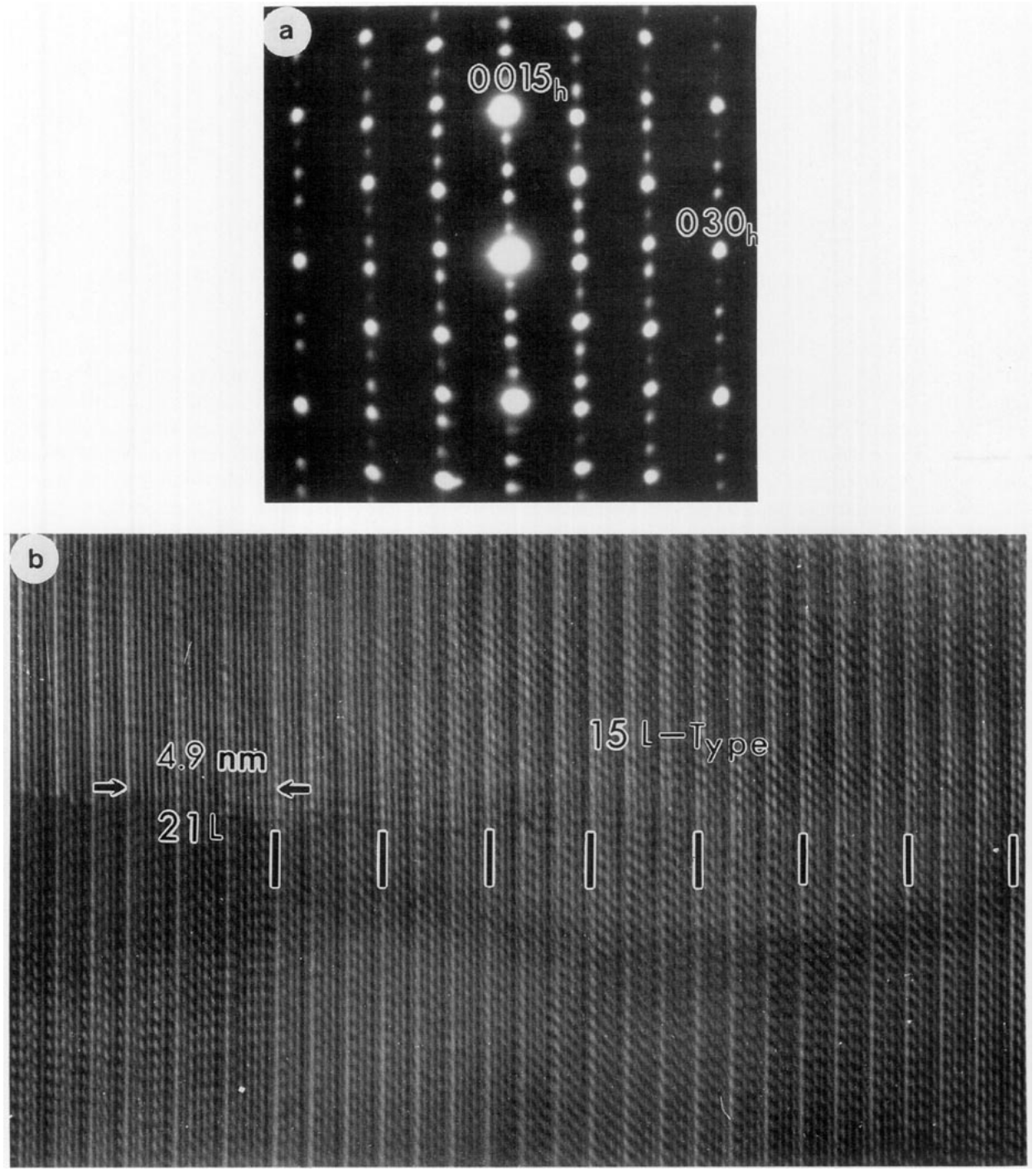

FIG. 10. (a) SAED pattern along $[100]_h$, corresponding to a crystal of the majority fraction of sample $BaMnO_{2.88}$. Weak streaking is observed along the c^*-axis. (b) Corresponding low-resolution image. An isolated 21R unit cell is intergrown in a 15R matrix.

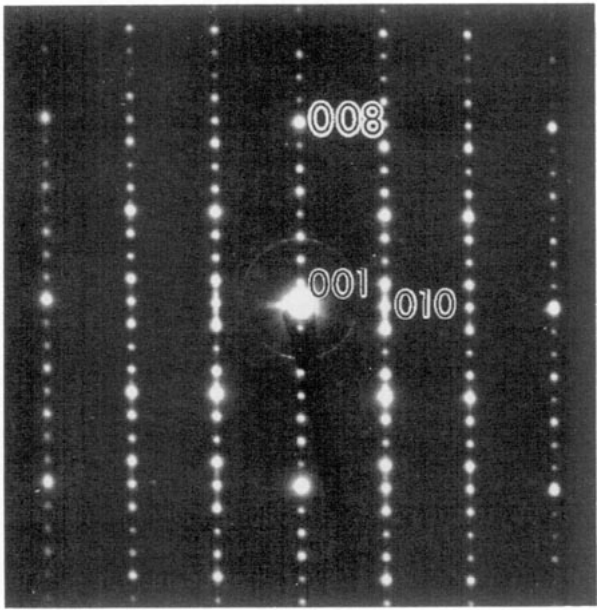

FIG. 11. SAED pattern corresponding to a 8H′-type structure along the $[100]_h$ zone axis.

this value, $BaMnO_{2.92}$, isolated crystals of the 21R type can be observed.

On the other hand, when the concentration of anionic vacancies increases ($y = 0.12$), some crystals showing hexagonal symmetry of the 8H′structural type appear, whose theoretical composition is $BaMnO_{2.875}$. In order to isolate this phase, further reduction is necessary.

Note that regarding all $BaMnO_{3-y}$ types reported thus far, this is the first finding of a rhombohedral phase in the $0 < y < 0.10$ compositional range, since only 2H ($y = 0$) and 15R ($y = 0.10$) structural types have been previously described. This is probably because the only systematic research performed on this system is that of Negas and Roth (*2*), which characterized the samples by power X-ray diffraction. To distinguish both 15R and 21R types, which show similar XRD patterns and, besides, usually appear as disordered intergrowths, the use of a microstructural characterization by HREM is required. To isolate the new 21R-type structure more work is in progress.

ACKNOWLEDGMENTS

Financial support of CICYT (Spain) through Research Projects MAT 91-031 and MAT 93-0207 is acknowledged. We also thank A. García and E. Baldonodo for technical assistance.

REFERENCES

1. A. Hardy, *Acta Crystallogr.* **15,** 179 (1962).
2. T. Negas and S. Roth, *J. Solid State Chem.* **3,** 323 (1971).
3. M. Parras, J. Alonso, J. M. González-Calbet, and M. Vallet-Regí, *Solid State Ionics* **106,** 614 (1993).
4. J. M. González-Calbet, M. Parras, J. Alonso, and M. Vallet-Regí, *J. Solid State Chem.***106,** 99 (1993).
5. NCEMSS program, National Center for Electron Microscopy, Materials Center for Electron Microscopy, Materials and Chemical Science Division, Lawrence Berkeley, CA, 1989.
6. "International Tables for X-Ray Crystallography," Vol II, p. 342. Kinoch Press, Birmingham, 1959
7. H. M. Rietveld, *J. Appl. Crystallogr.* **2,** 65 (1969).